JCB

Supplemental material

Bertero et al., https://doi.org/10.1083/jcb.201902117

Provided online are six tables. Table S1 shows CRISPR/Cas9 off-target analysis. Table S2 shows differential gene expression analyses of RNA-seq data. Table S3 shows gene ontology analyses of RNA-seq data. Table S4 shows QC metrics of DNase Hi-C experiments. Table S5 shows A/B compartment analyses of Hi-C data. Table S6 shows ontology enrichment analyses of genes in lamin A/C–sensitive B compartments.

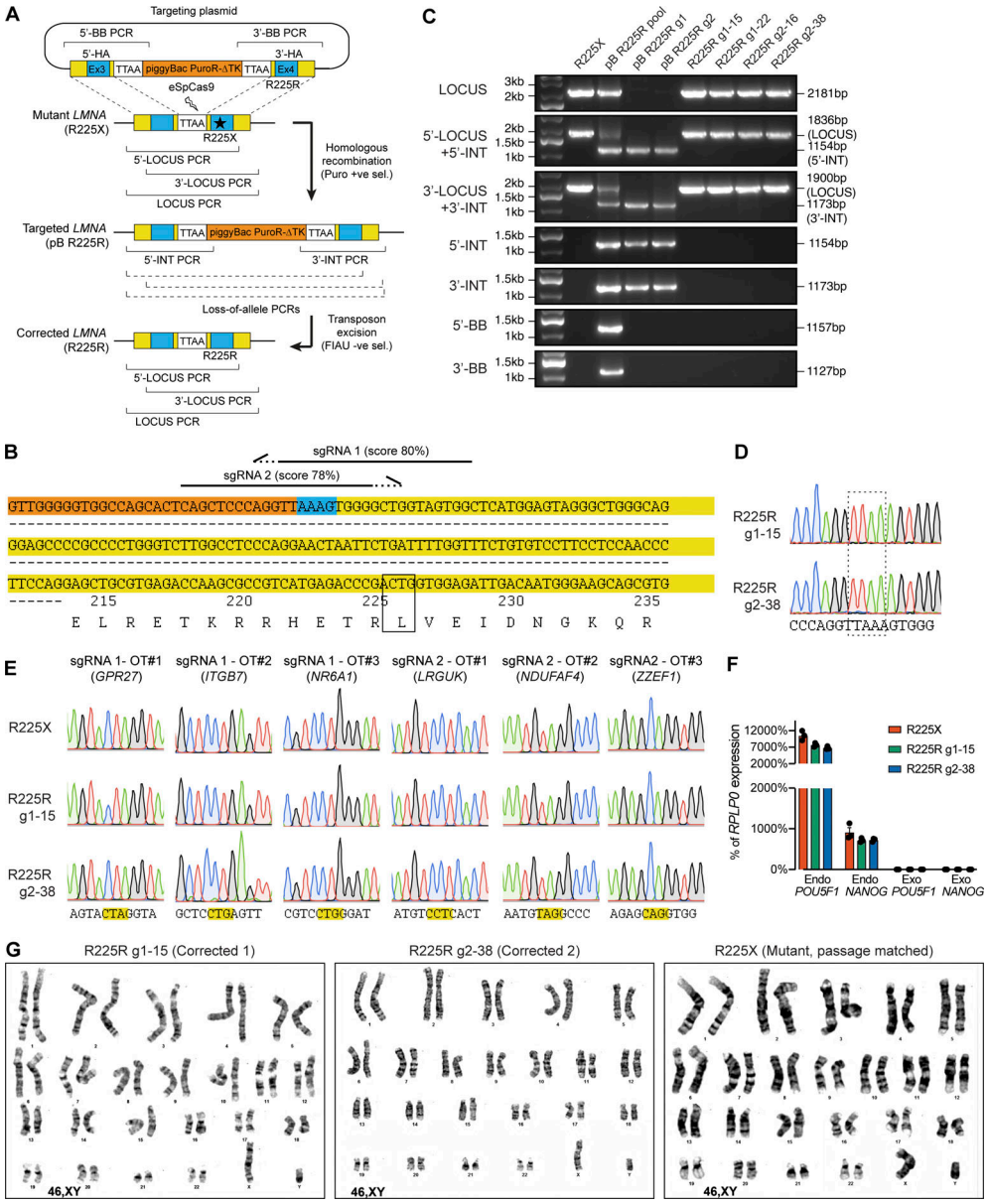

Figure S1. **Scarless correction of the LMNA R225X heterozygous mutation in hiPSCs. (A)** Schematics of the gene targeting and genotyping strategies. A targeting vector with wild-type up- and downstream homology arms (5′- and 3′-HA; Ex, exon) and a polycistronic piggyBac cassette carrying puromycin N-acetyltransferase and herpes simplex truncated thymidine kinase (PuroR-ΔTK) was used in combination with eSpCas9 to drive homologous recombination around an endogenous "TTAA" sequence proximal to the R225X mutation. Targeted clones were positively selected based on resistance to puromycin and screened by a panel of genomic PCR assays indicated by square brackets (PCR failing for gene-targeted alleles are indicated by dashed square brackets; see Materials and methods for details). The piggyBac cassette was subsequently excised using transposase leaving behind only a "TTAA" scar identical to the original sequence, and clones were negatively selected based on sensitivity to fialuridine (FIAU). Corrected clones were screened by genomic PCR, Sanger sequencing, and karyotyping. **(B)** Genomic sequence of the *LMNA* locus around the R225X mutation (highlighted by the box). The amino acid translation of portion of *LMNA* exon 4 is also reported. The location and directionality of the sgRNAs used for CRISPR/Cas9 targeting are indicated by the half arrows (dashed portion: PAM site; specificity scores are indicated). The 5′- and 3′-homology arms are shown with orange and yellow backgrounds, respectively. The "TTAA" sequence key to the scarless gene targeting strategy is shown with a blue background. **(C)** Selected genomic PCR results from the indicated hiPSC lines at different stages of the gene targeting procedure (see panel A). Pool, non-clonally selected hiPSCs after the first targeting step, providing a positive control for all PCR strategies. g1/g2, sgRNA1/sgRNA2 used for the first targeting step. **(D)** Sanger sequencing results for genomic PCR products of *LMNA* intron 3-exon 4 (LOCUS PCR) from the two corrected hiPSC clones selected for further experiments. The "TTAA" sequence was faithfully reconstituted following transposase excision of the piggyBac cassette (see Fig. 1 B for the R225R correction). **(E)** Sanger sequencing results for genomic PCR products of the indicated "high-risk" putative CRISPR/Cas9 off-target (OT) sites, as predicted by in silico analysis (Table S1). The PAM sites are highlighted in yellow. No CRISPR-associated mutation was identified. **(F)** RT-qPCR analysis for endogenous (endo) pluripotency genes *POU5F1* (*OCT4*) and *NANOG* compared to lentiviral-encoded exogenous (exo) transgenes delivered during hiPSC generation from skin fibroblasts. In agreement with previous results (Siu et al., 2012), exogenous transgenes were silenced following extensive passaging of R225X hiPSCs; lentiviral transgenes were not re-activated in corrected clonal hiPSC sublines (cycle threshold was undetectable in all three groups under the conditions tested based on 40 PCR cycles). n = 3 cultures; average ± SEM. **(G)** Representative G-banding karyotypes for the two corrected hiPSCs and passage-matched mutant hiPSCs, confirming a normal male 46 XY karyotype.

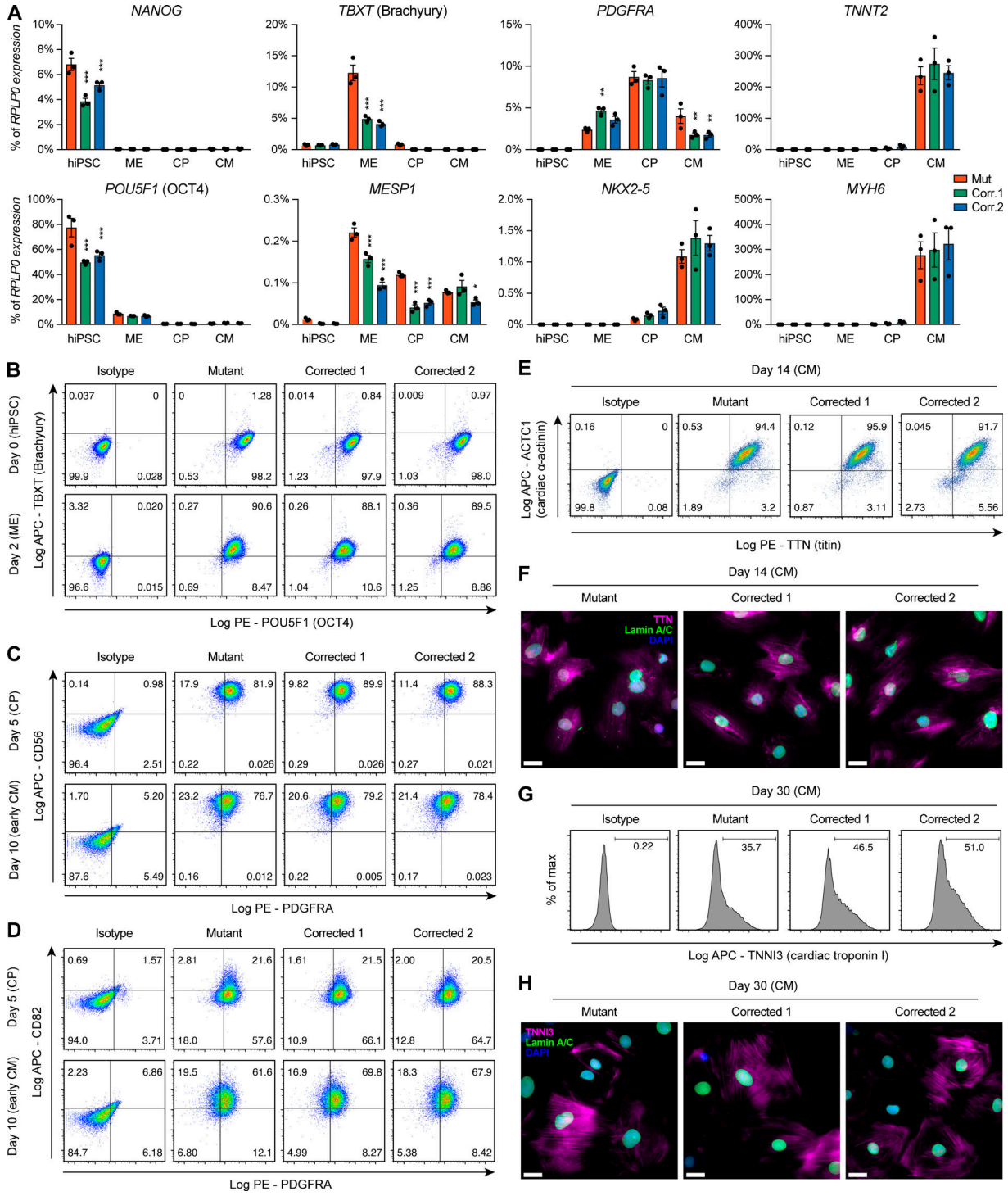

Figure S2. **Generation of lamin A/C haploinsufficient hiPSC-CMs. (A)** RT-qPCR analyses for lineage-specific markers at the indicated stages of hiPSC-CM differentiation (ME, mesoderm; CP, cardiac progenitor; CM, cardiomyocyte; see Fig. 1 C). Differences versus mutant were calculated by two-way ANOVA with post hoc Holm–Sidak binary comparisons (*, P < 0.05; **, P < 0.05; ***, P < 0.001; *n* = 3 differentiations; average ± SEM). **(B–E)** Representative flow-cytometry analyses at the indicated stages of hiPSC-CM differentiation. B reports expression of the pluripotency marker POU5F1 (OCT4) and of the mesoderm marker TBXT (Brachyury): compared to hiPSCs, ME cells express Brachyury and begin to down-regulate OCT4. C and D report expression of the cardiac mesoderm markers PDGFRA and CD56, and of the cardiomyocyte progenitor-fated marker CD82: as expected, CP are double-positive for PDGFRA and CD56, while CD82 appears in early CM at 10 d of differentiation. E reports expression of the sarcomeric proteins titin and cardiac α-actinin, confirming acquisition of CM identity by day 14 of differentiation. **(F)** Representative immunofluorescence on day 14 CM for the indicated proteins (nuclei counterstained with DAPI). Scale bars, 30 µm. **(G)** Representative flow-cytometry analysis for the adult cardiomyocyte marker cardiac troponin I, which replaces fetal slow-skeletal troponin I during cardiac maturation: this marker starts to be expressed in a proportion of day 30 hiPSC-CM. **(H)** Representative immunofluorescence on day 30 CM for the indicated proteins (nuclei counterstained with DAPI). Scale bars, 30 µm. Throughout the figure (and in all other supplemental figures), Mut or Mutant indicates *LMNA* R225X hiPSCs and Corr.1/2 or Corrected 1/2 indicate the two isogenic corrected control *LMNA* R225R hiPSCs.

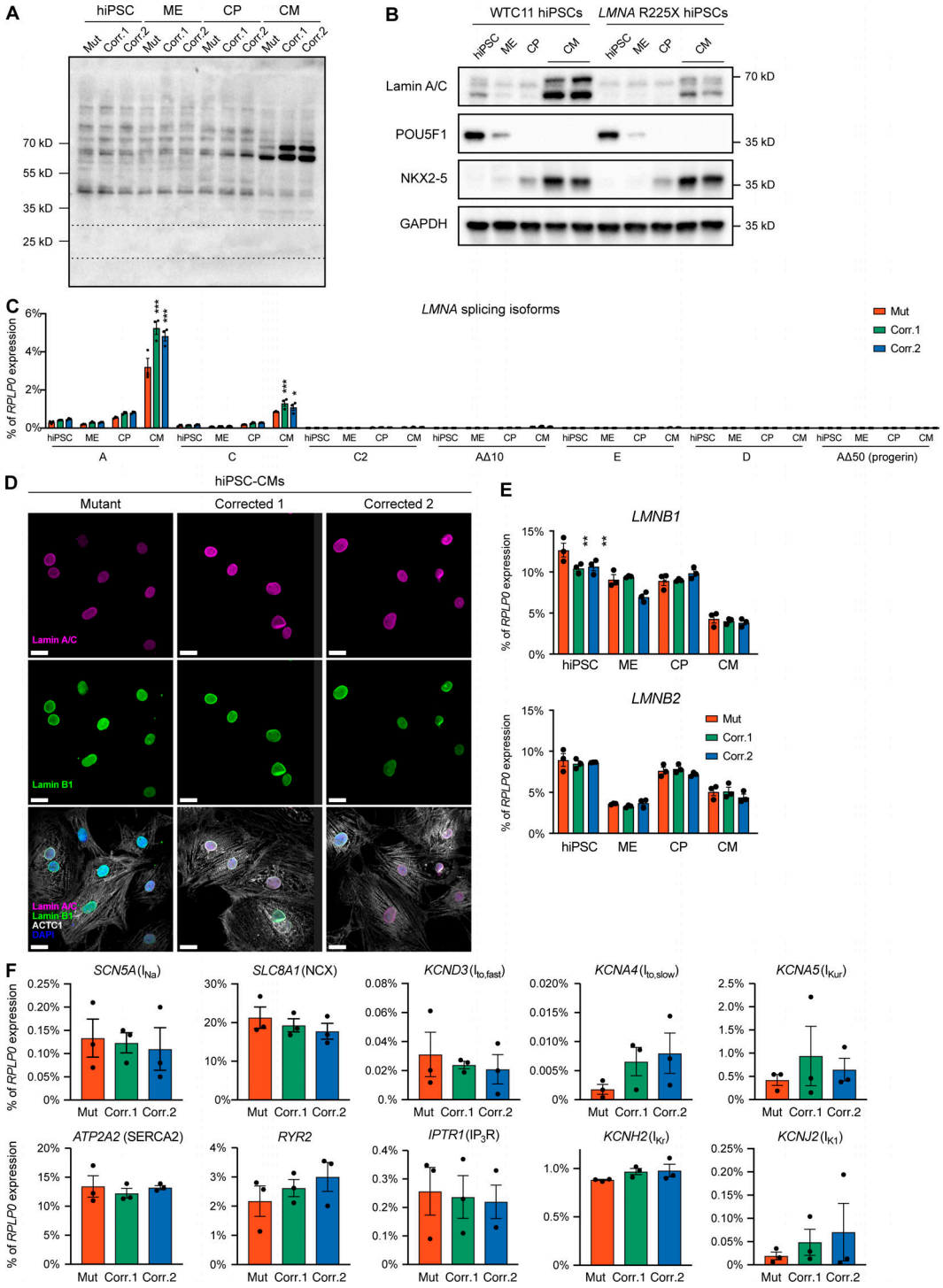

Figure S3. **Characterization of lamin A/C haploinsufficient hiPSC-CMs. (A and B)** Representative Western blots for lamin A/C and differentiation markers during iPSC-CM differentiation (see Fig. 1 C). In A, the uncropped image shows a stronger exposure of the same lamin A/C Western blot presented in Fig. 1 F. The expected location for putative truncated Lamin A and Lamin C due the R225X mutation is indicated by the dashed box (see Fig. 1 A), but no such truncation product could be detected. **(C)** RT-qPCR during hiPSC-CM differentiation for all splicing isoforms for the *LMNA* gene annotated on RefSeq (A: NM_170707.4; C: NM_005572.3; C2: NM_001282625.1; AΔ10: NM_170708.3; D: NM_001257374.3; E: NM_001282624.1; AΔ50: NM_001282626.2). Only lamin A and lamin C could be detected at substantial levels (>0.2% of the housekeeping gene *RPLP0*) in any of the groups. Differences versus mutant were calculated by two-way ANOVA with post hoc Holm–Sidak binary comparisons (*, $P < 0.05$; ***, $P < 0.001$; $n = 3$ differentiations; average ± SEM). **(D)** Representative immunofluorescence A- and B-type lamins in hiPSC-CM identified by co-staining for cardiac α-actinin (ACTC1; nuclei counterstained with DAPI). Scale bars, 20 µm. **(E)** RT-qPCR as described for panel C, but profiling expression of B-type lamins (**, $P < 0.01$; $n = 3$ differentiations; average ± SEM). **(F)** RT-qPCR in hiPSC-CMs at day 14 of differentiation to profile expression of the indicated ion-handling proteins involved in the cardiac action potential cycle (where relevant, the corresponding ion current is indicated). No significant differences were detected versus mutant (two-way ANOVA with post hoc Holm–Sidak binary comparisons; $n = 3$ differentiations; average ± SEM).

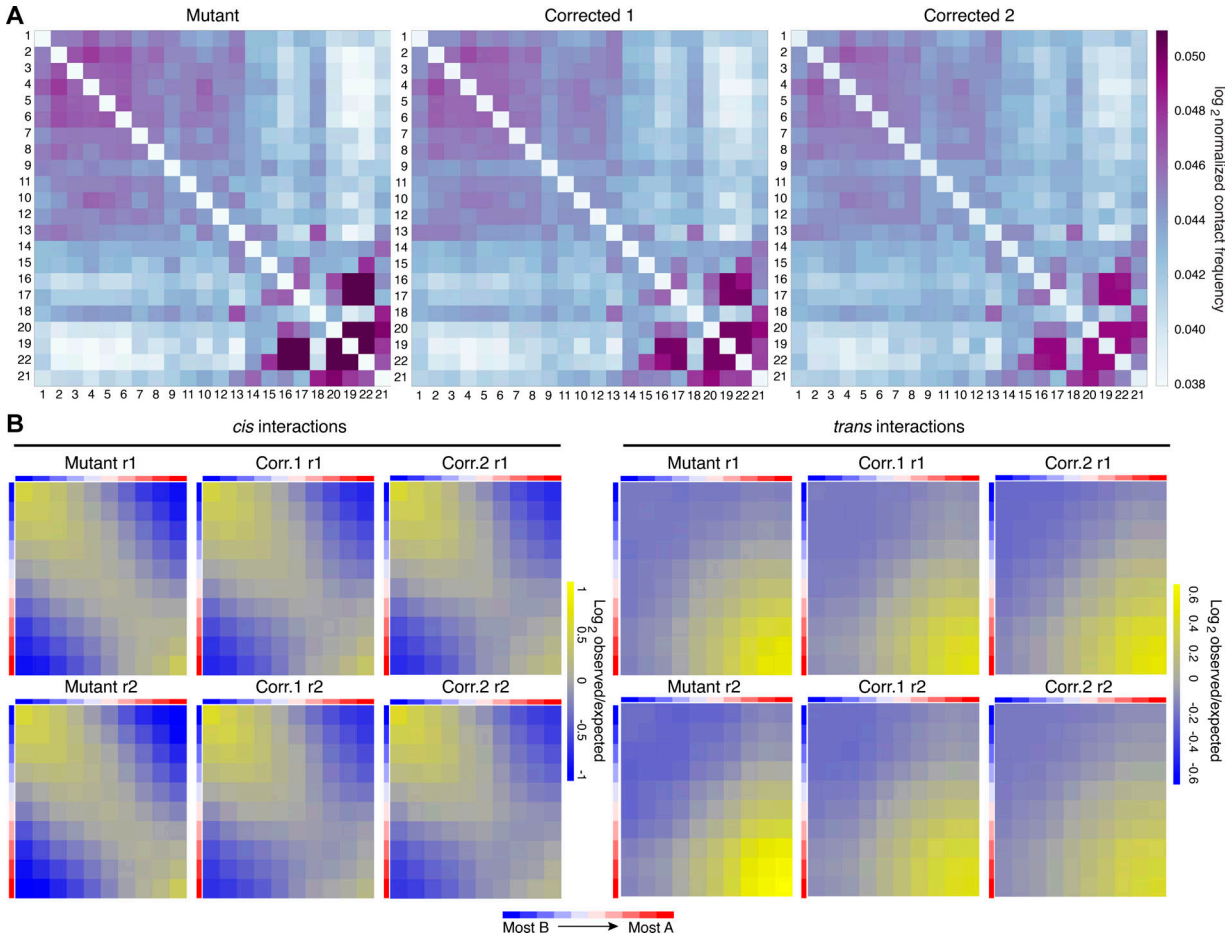

Figure S4. **Global properties of chromatin topology in lamin A/C haploinsufficient hiPSC-CMs. (A)** Representative heatmaps of contact matrices between chromosomes. Autosomes are ranked based on their size from left to right and top to bottom. **(B)** Heatmaps of cis or trans interactions between active (A) and inactive (B) chromatin compartments. 500-kb genomic bins were assigned to 10 deciles based on their PC1 score from the linear dimensionality reduction of the Hi-C matrix (from most B to most A; Table S5), and average observed/expected distance normalized scores for each pair of deciles were calculated. r1/r2, biological replicate 1/2 (independent differentiations).

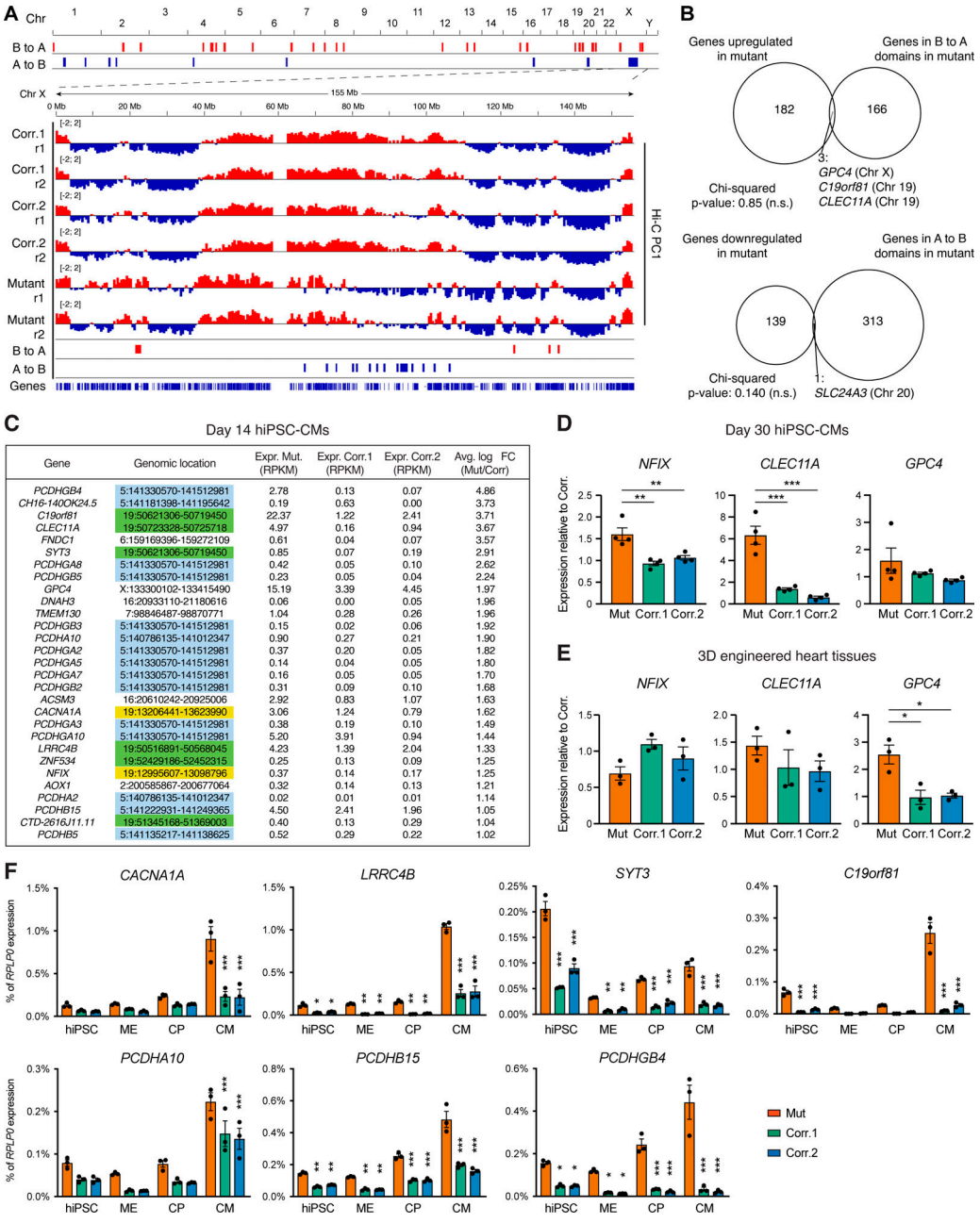

Gene	Genomic location	Expr. Mut. (RPKM)	Expr. Corr.1 (RPKM)	Expr. Corr.2 (RPKM)	Avg. log FC (Mut/Corr)
PCDHGB4	5:141330570-141512981	2.78	0.13	0.07	4.86
CH16-140OK24.5	5:141181398-141195642	0.19	0.63	0.00	3.73
C19orf81	19:50621306-50719450	22.37	1.22	2.41	3.71
CLEC11A	19:50723328-50725718	4.97	0.16	0.94	3.67
FNDC1	6:159169396-159272109	0.61	0.04	0.07	3.57
SYT3	19:50621306-50719450	0.85	0.07	0.19	2.91
PCDHGA8	5:141330570-141512981	0.42	0.05	0.10	2.62
PCDHGB5	5:141330570-141512981	0.23	0.05	0.04	2.24
GPC4	X:133300102-133415490	15.19	3.39	4.45	1.97
DNAH3	16:20933110-21180616	0.06	0.00	0.05	1.96
TMEM130	7:98846487-98870771	1.04	0.28	0.26	1.96
PCDHGB3	5:141330570-141512981	0.15	0.02	0.06	1.92
PCDHA10	5:140786135-141012347	0.90	0.27	0.21	1.90
PCDHGA2	5:141330570-141512981	0.37	0.20	0.05	1.82
PCDHGA5	5:141330570-141512981	0.14	0.04	0.05	1.80
PCDHGA7	5:141330570-141512981	0.16	0.05	0.05	1.70
PCDHGB2	5:141330570-141512981	0.31	0.09	0.10	1.68
ACSM3	16:20610242-20925006	2.92	0.83	1.07	1.63
CACNA1A	19:13206441-13623990	3.06	1.24	0.79	1.62
PCDHGA3	5:141330570-141512981	0.38	0.19	0.10	1.49
PCDHGA10	5:141330570-141512981	5.20	3.91	0.94	1.44
LRRC4B	19:50516891-50568045	4.23	1.39	2.04	1.33
ZNF534	19:52429186-52452315	0.25	0.13	0.09	1.25
NFIX	19:12995607-13098796	0.37	0.14	0.17	1.25
AOX1	2:200585867-200677064	0.32	0.14	0.13	1.21
PCDHA2	5:140786135-141012347	0.02	0.01	0.01	1.14
PCDHB15	5:141222931-141249365	4.50	2.41	1.96	1.05
CTD-2616J11.11	19:51345168-51369003	0.40	0.13	0.29	1.04
PCDHB5	5:141135217-141138625	0.52	0.29	0.22	1.02

Figure S5. **Chromatin compartment transitions and associated gene expression changes in lamin A/C haploinsufficient hiPSC-CMs. (A)** On the top, genome-wide view of 500-kb chromatin domains transitioning from B→A or A→B in corrected→mutant hiPSC-CMs (Table S5). On the bottom, genomic tracks of chromatin compartmentalization for chromosome X. Positive and negative Hi-C matrix PC1 scores are shown in red and blue, and indicate A and B compartments, respectively. **(B)** Overlap between genes up- or down-regulated in mutant hiPSC-CMs (RNA-seq on three differentiations; change greater than twofold; q-value < 0.05) and genes located in lamin A/C–sensitive chromatin compartments (Table S5). P-values for the significance of observed overlaps were calculated by chi-squared test (n.s., non-significant). **(C)** Average expression (Expr.) levels of genes found in lamin A/C–sensitive B chromatin compartments. Data are from the RNA-seq analyses of day 14 hiPSC-CMs (Table S2), and in contrast to panel B, all genes with an average fold-change (FC) greater than two for mutant versus corrected are reported (no filter by q-value). The genomic location of all genes is indicated, and colored backgrounds highlight genes found in three genomic hotspots where lamin A/C haploinsufficiency leads to compartment transitions from B to A, resulting in up-regulation of multiple genes located within (19p13.13, 19q13.33, and 5q31.3; see Fig. 6 E and Fig. 8 B). **(D and E)** RT-qPCR validation of gene expression changes in hiPSC-CMs matured by culture in vitro for 30 days (D) or by generation of 3D-EHTs (E). Differences versus mutant were calculated by one-way ANOVA with post hoc Holm–Sidak binary comparisons (*, P < 0.05; **, P < 0.01; ***, P < 0.001; *n* = 4 differentiations for panel D, and *n* = 3 3D-EHT batches for panel E; average ± SEM). **(F)** RT-qPCR during hiPSC-CM differentiation for genes found in lamin A/C–sensitive B compartments. All of these factors are not normally expressed at substantial levels (>0.2% of the housekeeping gene *RPLP0*) in control cells at any stage of differentiation, while they are up-regulated due to *LMNA* R225X mutation. With the exception of *SYT3*, up-regulation in mutant cells is observed specifically and/or with the strongest magnitude in hiPSC-CM, coincidentally with the lack of the developmental-associated transition to the B compartment of the chromatin regions containing these factors (Figs. 6 and 7). Differences versus mutant were calculated by two-way ANOVA with post hoc Holm–Sidak binary comparisons (*, P < 0.05; **, P < 0.01; ***, P < 0.001; *n* = 3 differentiations; average ± SEM).

Table S7. **Genotyping strategies for the characterization of CRISPR/Cas9-edited hiPSCs**

PCR	Primer	Sequence (5′- and -3′)	Location	Band wild type[a] (bp)	Band TARGET[b] (bp)	Band PLASMID[c] (bp)
LOCUS	LMNA_FW1	CCCCTGCTCAAACATCCTCA	Left to 5′ HAR	2,181	5,260 or loss-of-allele (LoA)	-
	LMNA_REV1	TGCAATCAGAGCTTCCCCAG	Right to 3′ HAR			
5′-INT	LMNA_FW1	CCCCTGCTCAAACATCCTCA	Left to 5′ HAR	-	1,154	-
	PB3-P2	GCGACGGATTCGCGCTATTTA GAAAG	5′ ITR			
5′-INT + 5′-LOCUS	LMNA_FW1	CCCCTGCTCAAACATCCTCA	Left to 5′ HAR	1,836	1,154 (5′-INT) and 4,915 or LoA (5′-LOCUS)	-
	PB3-P2	GCGACGGATTCGCGCTATTTA GAAAG	5′ ITR			
	LMNA_REV2	CTGTGGTTGTGGGGACACTT	3′ HAR			
3′-INT	PB5-P2	CGTCAATTTTACGCATGATTA TCTTTAAC	3′ ITR	-	1,173	-
	LMNA_REV1	TGCAATCAGAGCTTCCCCAG	Right to 3′ HAR			
3′-INT + 3′-LOCUS	LMNA_FW2	CCCAAAAGTACCCCAGGCAT	5′ HAR	1,900	1,173 (3′-INT) and 4,979 or LoA (3′-LOCUS)	-
	PB5-P2	CGTCAATTTTACGCATGATTA TCTTTAAC	3′ ITR			
	LMNA_REV1	TGCAATCAGAGCTTCCCCAG	Right to 3′ HAR			
5′-BB	M13-R49	GAGCGGATAACAATTTCACAC AGG	Plasmid 5′	-	-	1,157
	PB3-P2	GCGACGGATTCGCGCTATTTA GAAAG	5′ ITR			
3′-BB	PB5-P2	CGTCAATTTTACGCATGATTA TCTTTAAC	3′ ITR	-	-	1,127
	M13-F43	AGGGTTTTCCCAGTCACGACG TT	Plasmid 3′			

[a]Amplicon from the wild-type allele or from the corrected allele after excision of the piggyBac cassette.
[b]Amplicon from the gene-targeted allele after integration of the piggyBac cassette.
[c]Amplicon from the targeting plasmid after its random integration.

Table S8. **Genomic PCR primers for CRISPR/Cas9 off-target analysis**

Putative off-target (gene)	Forward primer (5′- and -3′)	Reverse primer (5′- and -3′)	Sequencing primer (5′- and -3′)	Amplicon size (bp)
sgRNA1 – OT#1 (*GPR27*)	TGTGCTTTGAGAAGCCCAGT	AGGCTATGTCAGGCCAACAC	TCTGGGCTCCTCTATCTTGG	1,563
sgRNA1 – OT#2 (*ITGB7*)	TGAGCTGTACCACGTTGCTG	CTTGCCAGTTACCAGGTCCC	GTGTCTACAGGGTGGTTAC	1,575
sgRNA1 – OT#3 (*NR6A1*)	ACACCCAACACAACGGGTAA	GAGGATTGAGCCACGTCCTT	CTACCCAGTATGCACACGAC	1,587
sgRNA2 – OT#1 (*LRGUK*)	ACAGATGCTTTCTCCCGGTC	AGCTTGGGCCTTTCACCTAC	GCAGATAATCCTGATGGTAGG	1,685
sgRNA2 – OT#2 (*NDUFAF4*)	TTTGAGTCGCAGCCTTCTGG	TGCCATGCTTGTTTCAAGGC	ATACCCAAGCAAATGCCTGG	1,507
sgRNA2 – OT#3 (*ZZEF1*)	TCACCCTACGGCTGTGTTTC	TGTACCAGGCCGTTTAGCTG	GGTTGACAGCATTGCTCATG	1,984

Table S9. **RT-qPCR primers**

Gene – isoform	Forward primer (5′- and -3′)	Reverse primer (5′- and -3′)	Amplicon size (bp)
ATP2A2	ATGGGGCTCCAACGAGTTAC	TTTCCTGCCATACACCCACAA	224
C19orf81	CCGAACGAGGAGGCCTGAC	AGTATCCACCCCCTCGAGCC	147
CACNA1A	AGGCATCCCTTTGATGGAGC	CTGAGTTTTGACCATGCGGC	222
CACNA1C	GCCGCTGCAGGAGAGTTTTA	CCCACATGTGCAAGACCACA	151
CLEC11A	TCCGGAATCTCCCTTCCCTT	TTATTGGCACCGGACCTAGC	156
GPC4	TGGACCGACTGGTTACTGATG	TGGTTTGCTGGTGTCAACCT	227
IPTR1	CGGAGCAGGGTATTGGAACA	GGTCCACTGAGGGCTGAAACT	122
KCNA4	GCCAAACCCGAGTGATTCCT	AAGCACTTCACCGTTCCCC	156
KCNA5	TAAGGAAGAGCAGGGCACTC	TTGCTCTTGGCCTTGACGTT	174
KCND3	ACCACACTGGGATACGGAGA	TTCGAACTGCCTGTTTTGGC	221
KCNH2	CAGCTCAACAGGCTGGAGAC	CTTCTTGGGGAAGCTCTGGG	250
KCNJ2	GTGCGAACCAACCGCTACA	CCAGCGAATGTCCACACAC	234
KCNQ1	AGCCTCACTCATTCAGACCG	TCTCCAGGAGTCACCCCATT	192
LMNA – A	CCATCACCACCACGGCTC	GTGACCAGATTGTCCCCGAA	243
LMNA – AΔ10	AACTCCACTGGGGAAGGCT	GAGTGACCGTGACACTGGAG	187
LMNA – AΔ50	ACGACGAGGATGAGGATGGA	TTCTGGGGGCTCTGGGCT	175
LMNA – C	CAACTCCACTGGGGAAGAAGTG	CGGCGGCTACCACTCAC	123
LMNA – C2	TCGGCAGAGAAGACAAAGCC	ATCAAGTCTCCCAGTCGGTG	209
LMNA – D	AATCTGGTCACCCGCTCCTA	CCCATCTCTTGTATGATGCTGC	86
LMNA – E	AGGGCTGATTTGCCAGTGATG	GCTATCAGGTCACCCTCCTTC	217
LMNB1	AGAACTGATGGAAAGCCGCA	CTTCAACCTCTCTTCTTCGCCT	295
LMNB2	CGGCTCCTGCTCAAGATCTCA	TTCTTGGCGCTCTTGTTGACC	194
LRRC4B	GGGCATTGCTCTTCCTCTGG	CGGATCACCTGGATGCCGTT	241
MESP1	TCGAAGTGGTTCCTTGGCAGAC	CCTCCTGCTTGCCTCAAAGTGTC	163
MYH6	GCCCTTTGACATTCGCACTG	GGTTTCAGCAATGACCTTGCC	103
NANOG (endo)	TTTGTGGGCCTGAAGAAAACT	AGGGCTGTCCTGAATAAGCAG	116
NANOG (exo)	TCAAGCCTCAGACAGTGGTTC	GGCCCGATTCCTGGCCCTCA	Not determined (Siu et al., 2012)
NFIX	ACAGCAGTCTCAGTCCTGGT	GGGCTGGGGGATTTTTCCAT	119
NKX2-5	GAGCCGAAAAGAAAGCCTGAA	CACCGACACGTCTCACTCAG	149
PCDHA10	GGAAGCTGCTGGATCGTGAA	AATCAGAAGCGTTGAGCCGT	216
PCDHB15	CTGACGGGAGGCTCTGAAAG	CAGACGGTCGGAAAGCTACA	132
PCDHGB4	AGCAGCACTGCACAGATACA	CCCGGGTACACGTTTTCTGA	107
PDGFRA	GCTCACTTCACTCTCCCCAAAG	CCGGCGTTCCTGGTCTTAG	153
POU5F1 (endo)	GGGTTCTATTTGGGAAGGTAT	TTCATTGTTGTCAGCTTCCT	131
POU5F1 (exo)	TCAAGCCTCAGACAGTGGTTC	CTTCAAAGCAAGGCAAGCTT	Not determined (Siu et al., 2012)
RPLP0	GGCGTCCTCGTGGAAGTGAC	GCCTTGCGCATCATGGTGTT	255
RYR2	ACAACAGAAGCTATGCTTGGC	GAGGAGTGTTCGATGACCACC	250
SCN5A	AACGGCACCTCTGATGTGTT	ACCTGAGGGTCTGCTGATAGA	199
SLC8A1	AGACCTGGCTTCCCACTTTG	TGGCAAATGTGTCTGGCACT	101
SYT3	GACTACGACTGCATCGGGCA	TGCTGCCTTTTGTGAAGCTG	178
TBXT	CAAATCCTCATCCTCAGTTTG	GTCAGAATAGGTTGGAGAATTG	143
TNNT2	TTCACCAAAGATCTGCTCCTCGCT	TTATTACTGGTGTGGAGTGGGTGTGG	166

Video 1. **Spontaneous contractions of mutant hiPSC-CMs.** Spontaneous contractions of mutant hiPSC-CM monolayers at day 14 of differentiation. Phase-contrast images were acquired at 30 fps and are shown at 30 fps.

Video 2. **Spontaneous contractions of corrected hiPSC-CMs.** Spontaneous contractions of corrected control hiPSC-CM monolayers (from Corr.1 hiPSCs) at day 14 of differentiation. Phase-contrast images were acquired at 30 fps and are shown at 30 fps.

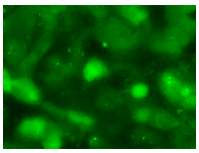

Video 3. **Calcium fluxes indicated by Fluo-4 fluorescence in monolayers of mutant hiPSC-CMs electrically paced at 1 Hz.** Calcium fluxes in electrically paced (1 Hz) mutant hiPSC-CM monolayers at day 30 of differentiation. Fluo-4 epifluorescence images were acquired at 20 fps and are shown at 20 fps.

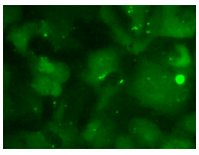

Video 4. **Calcium fluxes indicated by Fluo-4 fluorescence in monolayers of corrected hiPSC-CMs electrically paced at 1 Hz.** Calcium fluxes in electrically paced (1 Hz) corrected control hiPSC-CM monolayers (from Corr.1 hiPSCs) at day 30 of differentiation. Fluo-4 epifluorescence images were acquired at 20 fps and are shown at 20 fps.

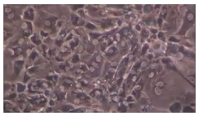

Video 5. **CCQ analyses in monolayers of mutant hiPSC-CMs electrically paced at 1 Hz.** Contractions of electrically paced (1 Hz) mutant hiPSC-CM monolayers at day 30 of differentiation. Phase-contrast images were acquired at 30 fps and are shown at 30 fps. Superimposed white arrows indicate the displacement vectors calculated by CCQ analysis.

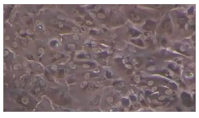

Video 6. **CCQ analyses in monolayers of corrected hiPSC-CMs electrically paced at 1 Hz.** Contractions of electrically paced (1 Hz) corrected control hiPSC-CM monolayers (from Corr.1 hiPSCs) at day 30 of differentiation. Phase-contrast images were acquired at 30 fps and are shown at 30 fps. Superimposed white arrows indicate the displacement vectors calculated by CCQ analysis.

Video 7. **Contractions of 3D-EHTs from mutant hiPSC-CMs.** Contractions of electrically paced (1 Hz) mutant 3D-EHTs analyzed 4 wk after casting. Phase-contrast images were acquired at 65 fps and are shown at 65 fps.

Video 8. **Contractions of 3D-EHTs from corrected hiPSC-CMs.** Contractions of electrically paced (1 Hz) corrected control 3D-EHTs (from Corr.1 hiPSCs) analyzed 4 wk after casting. Phase-contrast images were acquired at 65 fps and are shown at 65 fps.

Reference

Siu, C.W., Y.K. Lee, J.C.Y. Ho, W.H. Lai, Y.C. Chan, K.M. Ng, L.Y. Wong, K.W. Au, Y.M. Lau, J. Zhang, et al. 2012. Modeling of lamin A/C mutation premature cardiac aging using patient-specific induced pluripotent stem cells. *Aging (Albany N.Y.)*. 4:803–822. https://doi.org/10.18632/aging.100503